Effects of Averaging and Separating Soil Moisture and Temperature in the Presence of Snow Cover in a SVAT and Hydrological Model for a Southern Ontario, Canada, Watershed

S. R. FASSNACHT

Watershed Science, Colorado State University, Fort Collins, Colorado

Z.-L. YANG

Geological Sciences, University of Texas at Austin, Austin, Texas

K. R. SNELGROVE

Civil Engineering, University of Manitoba, Winnipeg, Manitoba, Canada

E. D. SOULIS AND N. KOUWEN

Civil Engineering, University of Waterloo, Waterloo, Ontario, Canada

(Manuscript received 4 November 2004, in final form 21 September 2005)

ABSTRACT

The energy and water balances at the earth's surface are dramatically influenced by the presence of snow cover. Therefore, soil temperature and moisture for snow-covered and snow-free areas can be very different. In computing these soil state variables, many land surface schemes in climate models do not explicitly distinguish between snow-covered and snow-free areas. Even if they do, some schemes average these state variables to calculate grid-mean energy fluxes and these averaged state variables are then used at the beginning of the next time step. This latter approach introduces a numerical error in that heat is redistributed from snow-free areas to snow-covered areas, resulting in a more rapid snowmelt. This study focuses on the latter approach and examines the sensitivity of soil moisture and streamflow to the treatment of the soil state variables in the presence of snow cover by using WATCLASS, a land surface scheme linked with a hydrologic model. The model was tested for the 1993 snowmelt period on the Upper Grand River in Southern Ontario, Canada. The results show that a more realistic simulation of streamflow can be obtained by keeping track of the soil states in snow-covered and snow-free areas.

1. Introduction

Numerous observational studies (Walsh 1984; Robock et al. 2003) and climate model simulations have shown that snow cover affects atmospheric circulation, air temperature, and the hydrologic cycle (Cohen and Rind 1991; Roesch 2003). Snow cover, especially fresh snow, has a much higher albedo than bare ground or liquid water, so that solar radiation absorption is significantly reduced, often as much as 50%. Where global warming has regional implications—for example, where the duration of snow cover is diminishing over time—the ground could be warmer, and, as a result, there is more heating of the atmosphere. This may further influence snow cover depletion and strengthen the global warming. Conversely, because of the insulating effects of snow, Stieglitz et al. (2003) demonstrated that over a 15-yr period increasing snow cover on the North Slope of Alaska warmed permafrost temperatures by as much as 1°C at 20-m depth.

Soil–vegetation–atmosphere transfer schemes (SVATs) have been used to represent land surface processes in atmospheric models. Most SVATs have simple representations of many of these processes (Yang et al. 1999), yet it remains an active research

Corresponding author address: Dr. S. R. Fassnacht, Watershed Science Program, Colorado State University, Fort Collins, CO 80523-1472.
E-mail: srf@cnr.colostate.edu

topic to understand what snow processes must be represented in the coupled SVAT and atmospheric models. Intercomparison studies have been used to identify the importance of snow albedo, fractional snow cover, and their interplay in controlling energy available for ablation (Slater et al. 2001). Physical representations of vertical snow processes have been shown to be important during transitional snow accumulation or depletion periods (Fassnacht and Soulis 2002). Horizontal hydrology is currently being incorporated in SVATs in the form of river routing (Arora et al. 1999; Soulis et al. 2000) and flow within grid cells (Soulis et al. 2000). However, few studies have examined how the treatment of soil temperature and moisture states, fractional snow cover, and their interplay impacts the streamflow.

Baker et al. (1991) measured the average snow depth required to fully mask the underlying surface and found that it was primarily a function of vegetation. The depletion of snow cover has been modeled using a relationship between snow depth and the ratio of snow-covered area (SCA) to the total area of a modeling grid block, which is often assumed to be linear between no SCA and zero depth to a minimum depth required to completely cover the ground referred to as the D_{100} (Verseghy 1991; Donald et al. 1995). A number of studies (Pomeroy et al. 1997; Hartman et al. 1999; Winstral et al. 2002) have shown that topography, in addition to vegetation, controls to a significant degree the distribution of snow depth. Yang et al. (1997) did not allow SCA to reach unity by incorporating the roughness length of the underlying soil or vegetation being covered with snow. This method is incorporated in many land surface schemes, but has been illustrated to underestimate SCA resulting in albedo lower than observations (Yang and Niu 2003). Roesch (2003) observed the same underestimation of SCA for flat terrain and an overestimation of SCA for alpine areas when computing SCA as a ratio of SWE to the sum of SWE and a critical snow depth, set at 0.01 m (Roesch et al. 2001).

This paper focuses on the energy and water mass balances for snow-covered and snow-free tiles of the land surface. This requires examination of the impacts of 1) numerical treatment of intertime step soil state variables (e.g., soil moisture, soil temperature), and 2) parameterization of areal snow cover, that is, fractional snow cover. Both are important to the modeling of land surface processes for climate and large-scale hydrological studies. While some models [e.g., the National Center for Atmospheric Research Land Surface Model 1 by Bonan (1996) and the Common Land Model by Dai et al. (2003)] have allowed each vegetation tile to carry soil state variables across time steps, there are no explicit studies of comparing such treatment versus the models that only carry the grid cell mean state variables. Few studies have documented the impacts of computing soil temperature and moisture for snow-covered and snow-free tiles separately. The impacts are presented herein.

2. Model

a. Linked land surface scheme—Hydrologic model

The Canadian Land Surface Scheme (CLASS), developed by Verseghy (1991, 2000) at the Meteorological Service of Canada (MSC), has been linked to the WATFLOOD hydrological model (Kouwen 1988), resulting in the WATCLASS model (Soulis et al. 2000). WATCLASS is a physically based model—that is, considering the water and energy balances—which has been used to generate multiyear streamflows. This model has been the focus of winter precipitation estimation (Fassnacht et al. 1999) and the representation of various winter processes (Fassnacht and Soulis 2002). A SVAT with a horizontal hydrological framework will enable the simulation of processes such as the redistribution of snow.

Vertically, the model uses three soil layers of variable depths and one snowpack layer for each grid cell. For each soil layer, temperature and soil moisture content (liquid and frozen) are the state variables. Soil heat is transferred by conduction and soil moisture is infiltrated according to Richard's equation. When there is excess water, after saturation has occurred in the second soil layer, this excess becomes interflow. Drainage from excess water in the bottom layer becomes groundwater flow. Groundwater enters the river system in the grid cell and is modeled with Darcy's law. Excess water in the top soil layer becomes overland flow, which is modeled used Manning's equation. Once the runoff reaches the stream channels, the streamflow is routed using a channel routing model.

For snow temperature, snow water equivalent (SWE), density, and albedo are used. Snow depth is computed from SWE and density, and the heat capacity and thermal conductivity are computed as a function of the snowpack density. Snowpack sublimation is computed using the bulk sensible and latent heat transfer formulas. This model divides the land cover into four vegetation types (coniferous, deciduous, crops, and grasses), bare ground, and water. Each land cover owns these state variables: soil temperature, moisture (liquid and frozen), and the growth index. From 30-m Landsat land cover data, a 10 km by 10 km modeling grid cell was divided in a fraction of one of six land-cover types (Kouwen et al. 1993). Within each of those fractions, the relative snow-covered and snow-free areas is computed based on snow depth relative to the land-cover-specific D_{100}.

There are various errors associated with a single snow layer model such as WATCLASS (Slater et al. 2001); however, this paper compares averaged with separated soil variables, which is also pertinent to multilayer models.

b. Snow-covered versus snow-free soil state variables

The extent of snow cover in WATCLASS is influenced by the D_{100} values for each land-cover type, similar to the use of coefficients of snow depth variation used by Pomeroy et al. (1998). While Donald et al. (1995) observed different D_{100} values for different land-cover types, 0.1 m is commonly used as the default (e.g., Verseghy 1991). Donald et al. (1995) illustrated that a linear snow cover depletion relationship yielded very similar results to a nonlinear relationship (e.g., Anderson 1973) for the WATFLOOD model, and thus a linear relationship was maintained in WATCLASS.

In the original WATCLASS model, the soil temperature and moisture (liquid and frozen water content) between snow-covered and snow-free areas were averaged from the area-weighted snow-covered and snow-free portions at the end of each time step in order to compute mass and heat fluxes. These average values were used as the values for the properties (temperature and moisture) at the beginning of the next time step. This resulted in a blending of the soil temperature and moisture during periods of partial snow cover; the warmer temperatures of the snow-free ground were averaged with the colder ground temperatures of the snow-covered areas, providing additional ground heat for snowmelt. This approach is hereafter referred to as AVRG. Energy and mass are conserved by partitioning both soil water content and temperature.

Specifically, for each layer the original AVRG approach averages the ice content, liquid water content, and soil temperature at the end of each time step based on snow-covered area and uses these averaged values as the state variables (ice content, liquid water content, and soil temperature) at the beginning of the next time step. For example, the average soil temperature, which is computed from the area-weighted snow-covered and snow-free portions at the end of a time step, is used as the soil temperature for both the snow-covered and snow-free areas at the beginning of the next time step. The same occurs for the soil moisture (ice and liquid).

In the second approach, the separation of the soil temperature and moisture between the snow-covered and snow-free areas from the end of a time step were used as the properties for the beginning of the next time step, therefore not changing the properties. This approach is referred to as SPRT. The soil temperature and moisture were maintained by not using the average values as approximations of the properties at the beginning of the next time step, as occurs for AVRG. The SPRT approach retained the separate soil state variables values for each snow-covered versus snow-free land-cover type. Since computation of average fluxes is still essential at the end of each time step, average fluxes were computed from the entire grid cell, that is, a weighted average of both the snow-covered and snow-free area. However, the individual soil temperature and moisture per land-cover type can be preserved for the next time step.

Both approaches preserve energy and mass for the snow-covered and snow-free areas. The SPRT approach does not change the soil temperature or moisture from the end of a time step to the beginning of the next time step. However, if there is snow but not complete snow cover—that is, 0 < SCA < 100%—the AVRG approach alters the energy and mass balance individually for the snow-covered area and for the snow-free area.

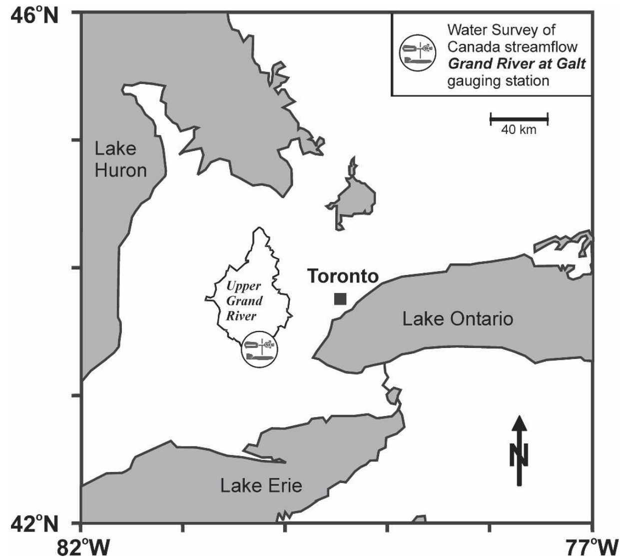

FIG. 1. Map of the study area.

3. Study area

Modeling was performed for the 3520-km^2 Upper Grand River in Southern Ontario, Canada (Fig. 1). The highest elevation in the basin is 535 m, with the outflow stream gauge at Galt (elevation of 290 m; location 43°21′10″N, 80°19′1″W). One-third of the annual precipitation (800~1000 mm) falls as snow and the snow-

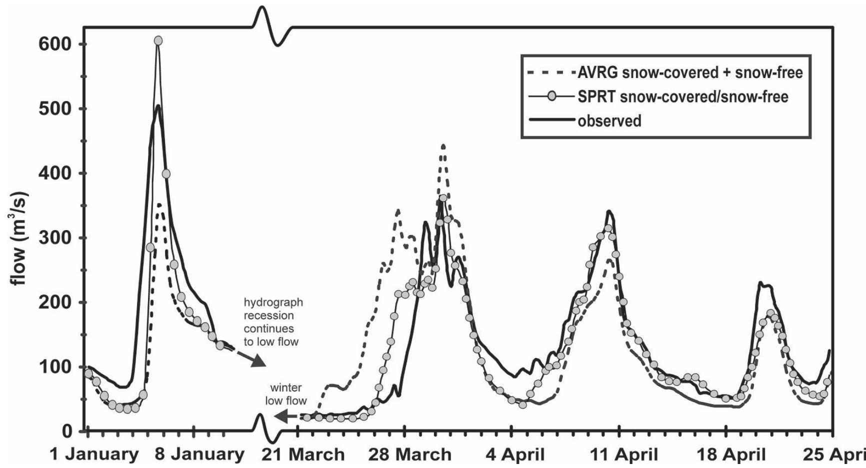

FIG. 2. Observed 1993 snowmelt hydrograph for the Grand River at Galt with hydrographs simulated using the AVRG soil temperature and moisture for snow-covered and snow-free areas and using the SPRT soil temperature and moisture for snow-covered and snow-free areas. The figure represents the early January 1993 rain on snow peak event and the spring snowmelt peak. Observed and simulated flows between the two peaks were the same.

melt begins in mid-March in the south and by mid-April in the north. Vegetation in the watershed is mostly cropland with some mixed deciduous–coniferous forest, and some wetland areas. See Fassnacht and Soulis (2002) for a more detailed description of the study basin.

4. Experimental design

Three experiments were performed to understand the impacts of the treatment of soil state variables for snow-covered and snow-free areas on the spring snowmelt hydrograph, the soil temperature, and liquid and solid soil water content. All experiments used the same WATCLASS version 2.7 model that was calibrated by Snelgrove (1996). The first two experiments assumed D_{100} = 0.1 m for all land-cover types, but differed in calculations of soil state variables. In the first experiment, we used the AVRG approach, and in the second experiment, we used the SPRT approach, as described in section 2b. The third experiment made use of SPRT and a series of tests with different D_{100} values. These values will be set to 0.1, 0.15, and 0.15 m everywhere except 0.06 m in the forest. They are called D_{100} = 0.1, D_{100} = 0.15, and D_{100} = 0.15/0.06$_{\text{forest}}$, respectively.

In all cases, the model was run from 1 January through 30 April 1993 because meteorological forcing data (e.g., temperature, precipitation, radiation, wind, humidity) were readily available. In 1993, the study area experienced a rain on snow event in early January and snowmelt runoff starting in late March. This winter was used because of limited availability of meteorological data in previous years, especially spatial precipitation data, and subsequent winters were warmer and the snowmelt runoff was much less significant. Also, the peak streamflow and basin-average peak SWE for 1993 were very close to the 1961 to 2000 average. Observed and simulated streamflow data were compared as hydrographs with a 6-h time step.

5. Results

a. *Impacts of the treatment of soil state variables*

The SPRT experiment yielded a hydrograph closer to the observed late March snowmelt streamflow hydrograph with the rising limb being only one day earlier, as compared to 2.5 days earlier (Fig. 2). The statistics comparing the simulated and observed snowmelt streamflow (Table 1) illustrate that while the net runoff volume for the entire snowmelt period (21 March to 25 April) is 7% lower for the SPRT than AVRG variables simulation due to the volume contributed by the early melt, the SPRT variables simulation matches the observed better than the AVRG variables simulation. After the first snowmelt streamflow peak, the magnitude of subsequent peaks is improved in the SPRT simulation. The initial snowmelt streamflow peak in the AVRG experiment is earlier than in the SPRT experiment since the ground heat associated with the soil temperature is averaged and thus provides more heat to melt the snow. Also, the water in the top soil layer melts faster for the snow-free area and slower for the snow-covered area in SPRT than in AVRG (Fig. 3).

The average daily air temperature increases to

TABLE 1. Statistics describing the relationship between the simulated (AVRG and SPRT variables) and observed snowmelt streamflow.

	Observed	Simulated (AVRG)	Simulated (SPRT)
Entire snowmelt period (21 Mar–25 Apr)			
Cumulative runoff (mm)	114.8	114.2	107.6
r^2	—	0.70	0.91
Root-mean-square error (mm)	—	47.9	32.2
Mean absolute error (mm)	—	66.1	33.6
Initial snowmelt peak (21 Mar–5 Apr)			
Cumulative runoff (mm)	39.7	57.4	39.3
r^2	—	0.70	0.88
Root-mean-square error (mm)	—	49.2	33.2
Mean absolute error (mm)	—	93.1	46.0

warmer than freezing on 22 March 1993 (Fig. 4a) and stays warmer than freezing for the remainder of the snowmelt season, except for one day (31 March). The temperature of the top 10-cm soil layer (Fig. 4b) lags behind the air temperature. In mid-April, when the ice begins to melt for the AVRG soil, the temperature increases, while the soil temperature of the under snow does not increase warmer than freezing for two additional days (Fig. 4b). This lag in warming corresponds to the lag in melting of ice (Fig. 3), and the difference in the ablation of snow (Fig. 5a). This difference is also illustrated in depletion of snow-covered area (Fig. 5b), which is intrinsically linked to the decrease in snow depth, as dictated by the D_{100} relationship. For forested areas, melt in the AVRG soil and under the snow cover of the SPRT soil occurs later than in open or low vegetation areas due to shading by the canopy.

Snowfall started to accumulate across portions the basin on 1 January (Fig. 5). On 4 January, the average daily air temperature increased to 8.7°C (Fig. 4a), which warmed the soil (Fig. 4b) under the thin snowpack, melting some of the frozen soil for the snow-free portion of SPRT (Fig. 3) while adding water to the soil for AVRG and the snow-covered portion of SPRT. This partial snowmelt was accompanied by rainfall that generated substantial runoff (Fig. 2). The simulated peak streamflow was 350 and 606 $m^3 s^{-1}$ for AVRG and SPRT versus an observed peak of 504 $m^3 s^{-1}$, while the runoff volume was underestimated by 35% and 17% for AVRG and SPRT. Since there was partial snow cover, the melting of soil moisture in the snow-free portion of SPRT contributed to runoff. Runoff is overestimated by SPRT since the D_{100} for accumulation period is likely less than for melting period (Davison 2004). This would yield less snow-free area, less frozen soil melt, and more infiltration. This could decrease the peak and, as infiltrated water flows through the near subsurface, that is, interflow, increase the receding limb of the hydrograph.

The averaging or blending of the soil temperature and moisture will transfer heat (and possibly liquid water) from the snow-free area to the snow-covered area. This will warm the soil below the snow cover, and will hasten melt. Similarly, ice can be melted because the warmer and possibly more liquid soil in the snow-free area will be blended with the colder, more frozen soil under the snow-covered area. When accumulating snow depths are shallow and encounter melt, such as

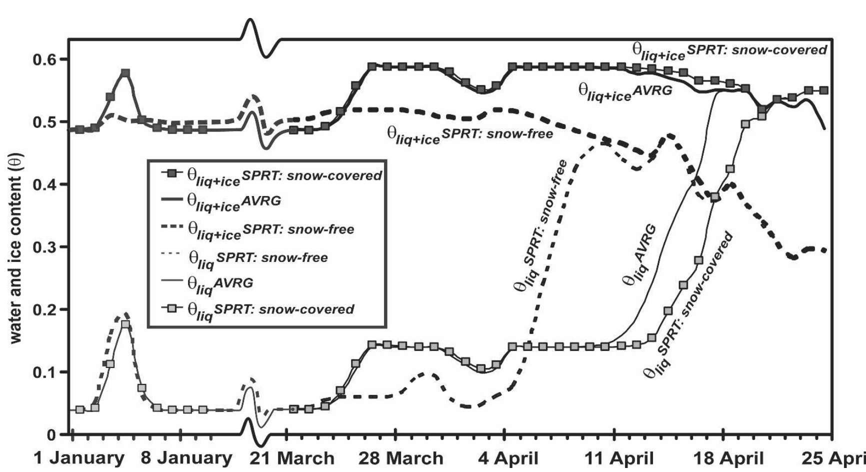

FIG. 3. Simulated top layer soil liquid and ice water content for the AVRG and SPRT experiments. The liquid water content is represented by the bottom three lines, whereas the ice (solid water) content is the difference between bottom and top lines. The water and ice content are constant from 8 January to 21 March.

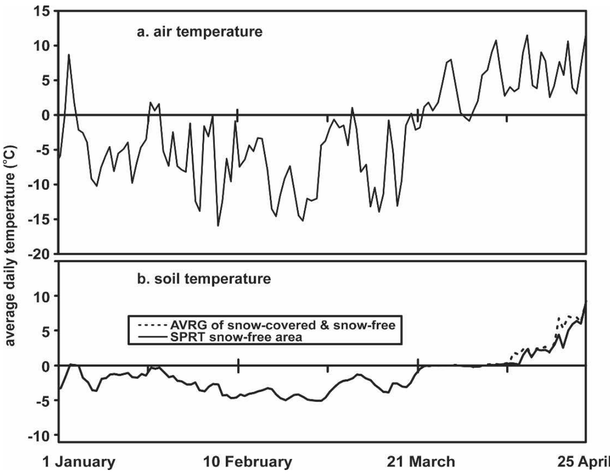

FIG. 4. (a) Observed air temperature, and (b) modeled top layer soil temperature for the AVRG and SPRT experiments.

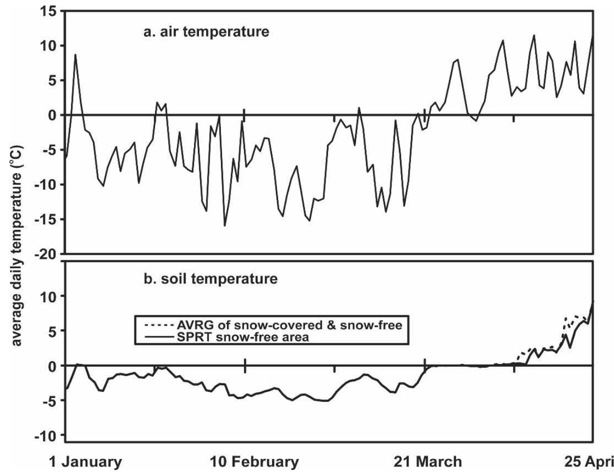

FIG. 5. Simulated AVRG and SPRT ratio of snow-covered area to total area for a low vegetation land cover subgrid cell.

occurred in early January, the AVRG experiment melted less ice than SPRT. Because of the averaging, the heat from the warmer soil in the snow-free area was transferred to the colder soil below the snow-covered area. Liquid water may also have been transferred from the snow-free soil to the snow-covered soil. This can melt snow, but in some situations will result in a decrease in ice melt in the snow-free area.

Air temperatures were warmer than freezing during 21–23 January. (Fig. 4a). This did not melt snow, but increased metamorphism of the snowpack and decreased the snow depth to below the D_{100} (Fig. 5).

b. Impacts of different D_{100} values

While the timing and shape of the rising and falling limbs of the hydrograph were the same, the magnitude of the first two peaks in the snowmelt hydrograph varied. For the first peak on 29 March, the peaks were 8%, 14%, and 9% less than observed for $D_{100} = 0.1$, $D_{100} = 0.15$, and $D_{100} = 0.15/0.06_{\text{forest}}$, and 13%, 25%, and 8% less than observed for the 30 March peak. Using different D_{100} values alters the exposure of snow-free areas. In the forested areas, snow-covered area was greatest for $D_{100} = 0.15/0.06_{\text{forest}}$ and least for $D_{100} = 0.15$, which made the snow depth less for $D_{100} = 0.15/0.06_{\text{forest}}$, since snowfall was constant for all scenarios. However, the differences were actually small since D_{100} was only a factor between a snow depth of 0.15 and 0.10 m (0.06 m for the forest scenario), which occurred during accumulation and ablation.

In the experiment presented herein, the D_{100} value was the same for accumulation and ablation. Davison (2004) tested different accumulation and ablation D_{100} values and found that the modeled snow variables were sensitive to the D_{100} value, as were estimated heat fluxes. For different land-cover types, ablation D_{100} values have been estimated from aerial photography, remote sensing, and field work (e.g., Donald et al. 1995). However, there are no field-based measurements of D_{100} in an accumulation setting.

6. Conclusions

We have examined, using WATCLASS, the impacts on streamflow of the numerical treatment of soil moisture (ice and liquid) and soil temperature for the three soil layers for snow-covered and snow-free fractions. In WATCLASS, when a modeling grid cell is partially snow covered, the soil moistures and temperatures are subsequently averaged to compute the sensible and latent heat fluxes from a modeling grid cell. These average soil variables are then used at the beginning of the next time step. This increases the temperature and liquid water content of soil under snow cover while decreasing the temperature and possibly increasing ice content of soil with no overlying snow. The separation of the soil state variables improves the spring snowmelt hydrograph by more closely simulating the timing and magnitude of the initial rising limb. For the separation of snow-covered and snow-free areas, some of the melt was delayed, as heat was not transferred directly from the bare ground to the soil below the snow cover. It is recommended that the values of the soil state variables be preserved between time steps. The use of different D_{100} values altered the magnitude of the simulated streamflow peaks by 6% to 17%.

Acknowledgments. This research was supported by Meteorological Service of Canada (MSC) Science Subventions, MSC-CCRNet Land-Air Node funding, and MSC-CRYSYS funding.

ZLY was supported under NASA Grant NAG5-12577. Dr. D. L. Verseghy of MSC provided the CLASS code. Thanks are also due to MSC-Climate Archive for providing the meteorological data, and Water Survey of Canada-Guelph for providing the hourly streamflow data. The comments from three anonymous reviewers helped clarify this paper.

REFERENCES

Anderson, E. A., 1973: National Weather Service River Forecast System—Snow Accumulation and Ablation Model. NOAA Tech. Rep. NWS Hydro-17, 217 pp.

Arora, V. K., F. H. S. Chow, and R. B. Grayson, 1999: A river flow routing scheme for general circulation models. *J. Geophys. Res.,* **104** (D12), 14 347–14 357.

Baker, D. G., R. H. Skaggs, and D. L. Ruschy, 1991: Snow depth required to mask the underlying surface. *J. Appl. Meteor.,* **3,** 387–392.

Bonan, G. B., 1996: A land surface model (LSM version 1.0) for ecological, hydrological, and atmospheric studies: Technical description and user's guide. NCAR Tech. Note NCAR/TN-417+STR, 150 pp.

Cohen, J., and D. Rind, 1991: The effects of snow cover on the climate. *J. Climate,* **4,** 689–706.

Dai, Y., and Coauthors, 2003: The Common Land Model. *Bull. Amer. Meteor. Soc.,* **84,** 1013–1023.

Davison, B. J., 2004: Snow accumulation in a distributed hydrological model. M.A.Sc. thesis, Dept. of Civil Engineering, University of Waterloo, 124 pp.

Donald, J. R., E. D. Soulis, N. Kouwen, and A. Pietroniro, 1995: A land cover-based snow cover representation for distributed hydrologic models. *Water Resour. Res.,* **31,** 995–1009.

Fassnacht, S. R., and E. D. Soulis, 2002: Implications during transitional periods of improvements to the snow processes in the Land Surface Scheme—Hydrological model WATCLASS. *Atmos.–Ocean,* **40,** 389–403.

——, ——, and N. Kouwen, 1999: Algorithm application to improve weather radar snowfall estimates for winter hydrologic modelling. *Hydrol. Processes,* **13,** 3017–3039.

Hartman, M. D., J. S. Baron, R. B. Lammers, D. W. Cline, L. E. Band, G. E. Liston, and C. Tague, 1999: Simulations of snow distribution and hydrology in a mountain basin. *Water Resour. Res.,* **35,** 1587–1603.

Kouwen, N., 1988: WATFLOOD: A micro-computer based flood forecasting system based on real-time weather radar. *Can. Water Res. J.,* **13,** 62–77.

——, E. D. Soulis, A. Pietroniro, J. R. Donald, and R. A. Harrington, 1993: Grouped response units for distributed hydrologic modeling. *J. Water Resour. Plann. Manage.,* **119,** 289–305.

Pomeroy, J. W., P. Marsh, and D. M. Gray, 1997: Application of a distributed blowing snow model to the Arctic. *Hydrol. Processes,* **11,** 1451–1464.

——, D. M. Gray, K. R. Shook, B. Toth, R. H. Essery, A. Pietroniro, and N. Hedstrom, 1998: An evaluation of snow accumulation and ablation processes for land surface scheme modelling. *Hydrol. Processes,* **12,** 2339–2367.

Robock, A., M. Q. Mu, K. Y. Vinnikov, and D. Robinson, 2003: Land surface conditions over Eurasia and Indian summer monsoon rainfall. *J. Geophys. Res.,* **108,** 4131, doi:10.1029/2002JD002286.

Roesch, A., 2003: A new snow cover parameterization for use in GCMs. *Snow Processes: Representation in Atmospheric and Hydrological Models: Proc. 2003 IUGG Workshop,* Sapporo Japan, IUGG.

——, M. Wild, H. Gilgen, and A. Ohmura, 2001: A new snow cover parameterization for the ECHAM4 GCM. *Climate Dyn.,* **17,** 933–946.

Slater, A., and Coauthors, 2001: The representation of snow in land-surface schemes: results from PILPS 2(d). *J. Hydrometeor.,* **2,** 7–25.

Snelgrove, K. R., 1996: Hydrologic computing modeling using the WATFLOOD hydrologic model and the Canadian Land Surface Scheme (CLASS). M.A.Sc. project, Dept. of Civil Engineering, University of Waterloo, 162 pp.

Soulis, E. D., K. R. Snelgrove, N. Kouwen, F. R. Seglenieks, and D. L. Verseghy, 2000: Toward closing the vertical water balance in Canadian atmospheric models: Coupling of the land surface scheme CLASS with the distributed hydrological model WATFLOOD. *Atmos.–Ocean,* **38,** 251–269.

Stieglitz, M., S. J. Déry, V. Romanovsky, and T. E. Osterkamp, 2003: The role of snow cover in the warming of Arctic permafrost. *Geophys. Res. Lett.,* **30,** 1721, doi:10.1029/2003GL017337.

Verseghy, D. L., 1991: CLASS—A Canadian Land Surface Scheme for GCMs: I. Soil model. *Int. J. Climatol.,* **11,** 111–133.

——, 2000: The Canadian Land Surface Scheme (CLASS): Its history and future. *Atmos.–Ocean,* **38,** 1–13.

Walsh, J. E., 1984: Snow cover and atmospheric variability. *Amer. Sci.,* **72,** 50–57.

Winstral, A., K. Elder, and R. E. Davis, 2002: Spatial snow modeling of wind-redistributed snow using terrain-based parameters. *J. Hydrometeor.,* **3,** 524–538.

Yang, Z.-L., and G.-Y. Niu, 2003: The versatile integrator of surface and atmosphere processes (VISA). Part I: Model description. *Global Planet. Change,* **38,** 175–189.

——, R. E. Dickinson, A. Robock, and K. Y. Vinnikov, 1997: Validation of the snow sub-model of the Biosphere–Atmosphere Transfer Scheme with Russian snow cover and meteorological observational data. *J. Climate,* **10,** 353–373.

——, and Coauthors, 1999: Simulation of snow mass and extent in general circulation models. *Hydrol. Processes,* **13,** 2097–2113.